

# Mode-Evolution-Based, Broadband 1x2 Port High-Pass/Low-Pass Filter for Silicon Photonics

Emir Salih Magden<sup>1\*</sup>, Christopher V. Poulton<sup>1</sup>, Nanxi Li<sup>1,2</sup>, Diedrik Vermeulen<sup>1</sup>, Alfonso Ruocco<sup>1</sup>, Neetesh Singh<sup>1</sup>, Gerald Leake<sup>3</sup>, Douglas Coolbaugh<sup>3</sup>, Leslie A. Kolodziejski<sup>1</sup>, and Michael R. Watts<sup>1</sup>

<sup>1</sup>Research Laboratory of Electronics, Massachusetts Institute of Technology, 77 Massachusetts Ave, Cambridge, MA 02139, USA

<sup>2</sup>John A. Paulson School of Engineering and Applied Science, Harvard University, 29 Oxford St, Cambridge, MA 02138, USA

<sup>3</sup>College of Nanoscale Science and Engineering, University at Albany, 1400 Washington Ave, Albany, NY 12222, USA

\*esm@mit.edu

**Abstract:** We demonstrate integrated, mode-evolution-based, 1x2 port high-pass/low-pass filters in a silicon photonics platform that can simultaneously achieve broadband operation, single cutoff wavelength, and a record high filter roll-off of 2.5 dB/nm for the first time.

**OCIS codes:** (130.7408) Wavelength filtering devices; (230.1360) Beam splitters; (130.3120) Integrated optics devices.

## 1. Introduction

To make use of the recent advances in spectral broadening [1], and new frequency generation techniques [2], on-chip integration of robust, broadband photonic filters is required. So far, for optical routing, manipulation, and spectrally separating or filtering broadband input signals, various integrated optical filters including multi-mode or Mach-Zehnder interferometers [3,4], as well as arrayed-waveguide and Bragg gratings have been used in the visible, near-infrared, mid-infrared regimes [5,6]. However, achieving broadband operation with single cutoff high-pass or low-pass responses and sharp roll-offs still remains a challenge, due to the interferometric behavior of these devices.

Broadband spectral splitting has been studied with the use of directional and adiabatic couplers [7,8]. These devices take advantage of the higher confinement factor at shorter wavelengths that effectively reduces the coupling strength to an adjacent waveguide, providing spectral selectivity. However, confinement-based devices like these fundamentally exhibit slow filter roll-offs, as they rely on waveguide dispersion along the length of the coupler. Here, we present an alternative, mode-evolution-based device that maintains the input in the fundamental transverse-electric (TE) mode throughout the whole structure. In contrast to devices using evanescent coupling, here the cutoff wavelength is determined by hybridization of modes in a two waveguide system, allowing for much sharper filter roll-offs, inherently broadband operation, and a more robust design methodology.

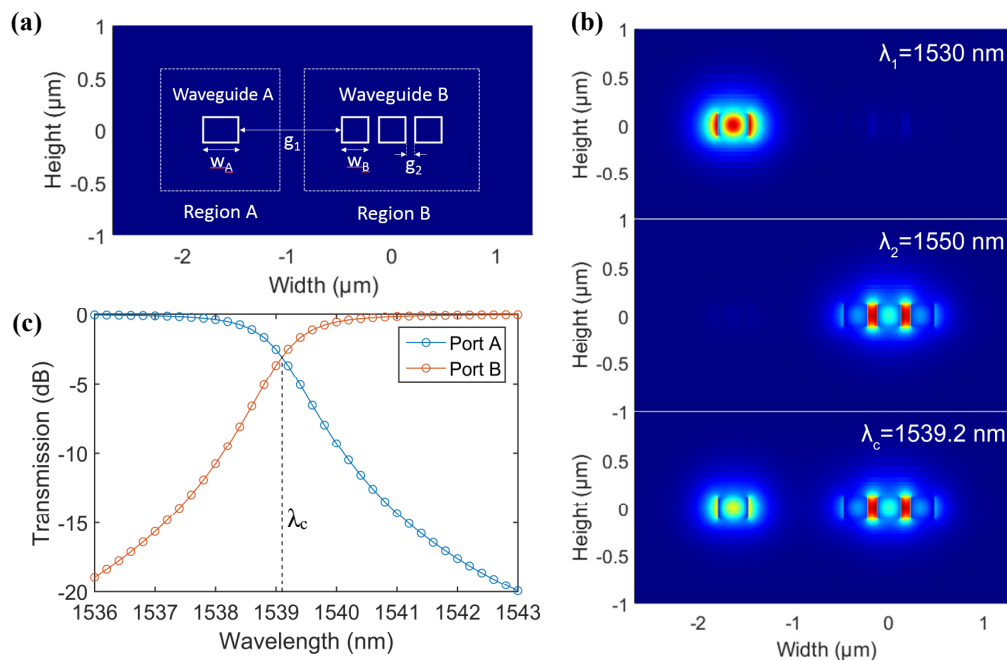


Fig. 1 (a) Design of waveguide cross-section for spatial separation of spectral components. (b) Fundamental TE mode electric fields for 1530 nm, 1550 nm, and 1539.2 nm. (c) Estimated transmission for the two output ports.

## 2. Theory and Design

The proposed device is a 1x2 high-pass/low-pass filter consisting of a mode-evolution-based adiabatic coupler. It can be used to separate a broadband input signal into a high-pass and a low-pass output port according to a designed cutoff wavelength ( $\lambda_c$ ). The two key elements of the proposed structure are the waveguide cross-section that separates the fundamental modes of the long and short wavelengths, and the transition that transforms the mode adiabatically from a single waveguide to this cross-section.

In a silicon photonics process with a single material core layer (such as Si, Si<sub>3</sub>N<sub>4</sub>, TiO<sub>2</sub>, or Al<sub>2</sub>O<sub>3</sub>) and high aspect-ratio waveguides, according to the solutions of the Helmholtz equation, the fundamental TE mode forms over the widest waveguide, given that the waveguides are sufficiently separated. However, if brought closer together, a group of waveguides can act as a single wider waveguide for longer wavelengths. This is the main design principle used in the waveguide cross-section shown in Fig. 1 (a), designed for a 220 nm silicon-on-oxide (SOI) platform with a 2 $\mu$ m top oxide cladding. Major components of the electric fields for the fundamental TE modes are given in Fig. 1 (b). For shorter wavelengths, the fundamental TE mode has the largest overlap with “waveguide A”, as this is the widest Si waveguide in the given window. On the other hand, for sufficiently long wavelengths, “waveguide B” acts as a single waveguide, and hence has the largest overlap with the fundamental TE mode. Cutoff is achieved when the first two eigenmodes of the designed cross-section have equal propagation constants. Using  $w_A = 318$  nm,  $w_B = 250$  nm, and  $g_2 = 100$  nm, the cutoff wavelength is expected to be around 1539.2 nm. At this wavelength, power is evenly divided between the two ports as shown by the electric field profile. Moreover, transmission spectrum for each port can be estimated by the ratios of the Poynting vector flux through Regions A and B in Fig. 1 (a) to the total flux. These are plotted as a function of wavelength in Fig. 1 (c).

After the cross-section is determined, transition components for mode evolution from a single-mode waveguide input to the desired cross-section are designed. The three segments in this transition are shown in Fig. 2 (a). First, the single-mode input waveguide on the left is evolved into a three-piece waveguide with widths  $w_B$  and gaps  $g_2$ . In the second segment of the transition, a new waveguide is tapered from the minimum allowed width to a width of  $w_A$ , with a separation of  $g_1$  from the adjacent group of three waveguides. The third segment of the transition slowly separates waveguides A and B, allowing for short and long wavelengths to be isolated while minimizing crosstalk between the two outputs. The choice of  $g_1$  presents a tradeoff between the lengths of segments 2 and 3. Here,  $g_1 = 200$  nm in segment 2, and is tapered up to 1  $\mu$ m by the end of segment 3 for sufficient spectral separation within a total device length of 1.5 mm. After the transition structures, “waveguide B” is evolved back to a single waveguide using an identical transition in reverse. Both outputs are then tapered to appropriate widths for single-mode guiding. According to the eigenmode expansion simulation results in Fig. 2 (b-d), for transmission to the fundamental TE mode with minimum loss, the lengths of transition segments were chosen as  $L_1 = 200$   $\mu$ m,  $L_2 = 260$   $\mu$ m, and  $L_3 = 900$   $\mu$ m for the C-band device.

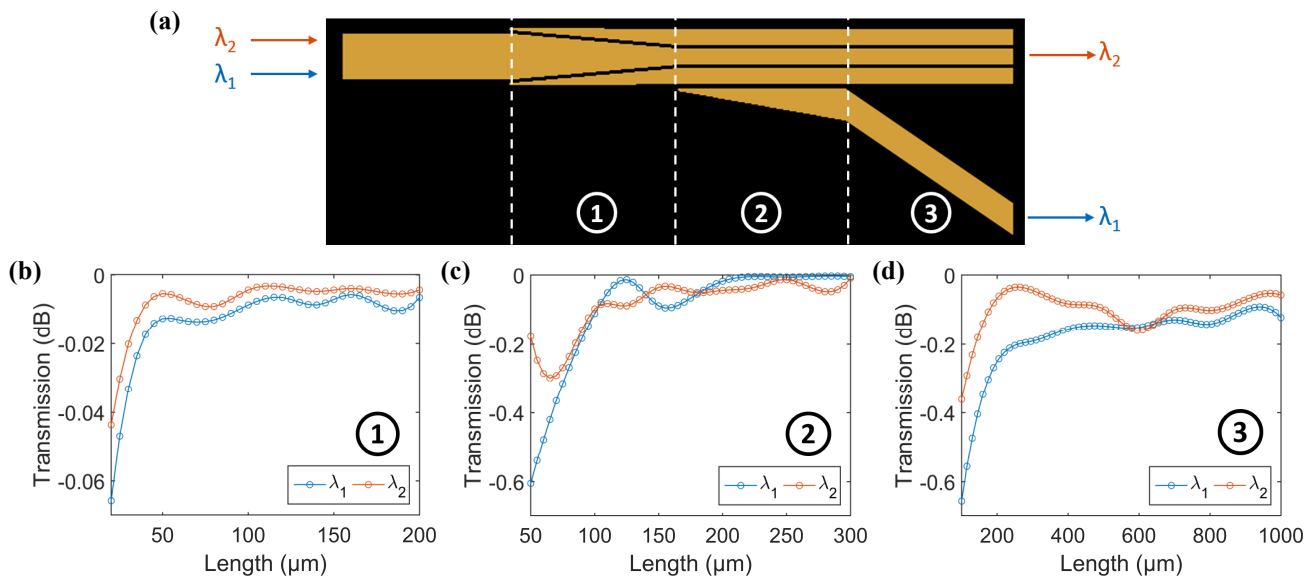


Fig. 2 (a) Schematic view of the transition components to the previously designed cross-section (not to scale). Corresponding eigenmode expansion simulation results for transmission between fundamental TE modes through (b) Segment 1, (c) Segment 2, and (d) Segment 3 for  $\lambda_1 = 1530$  nm and  $\lambda_2 = 1550$  nm

### 3. Results and Discussion

Using the described methodology, two sets of 1x2 filters were designed for cutoff wavelengths of 1540 nm and 2120 nm. For each set of devices,  $w_A$  was varied by  $\pm 6$  nm and  $\pm 8$  nm respectively to observe the resulting cutoff shift. Devices were fabricated in a standard CMOS process using 193 nm immersion lithography on 300 mm SOI wafers. Filter responses were characterized using polarization controlled input signals from numerous continuous wave lasers ranging from 1.46  $\mu\text{m}$  to 2.40  $\mu\text{m}$ . The transmission spectra in Fig. 3 (a) shows consistent device performance for filters with cutoffs in the 1550 nm window. Less than 1 dB insertion loss,  $\sim 10$  dB extinction ratio, and 2.5 dB/nm filter roll-off were obtained. For  $w_A = 318$  nm, the measured cutoff wavelength of 1533 nm was only slightly off from the design target of 1539 nm, where the difference can be attributed to thickness and width variations due to fabrication. Cutoff wavelengths ranging from 1495 nm to and 1575 nm were achieved by incrementing  $w_A$  in steps of 6 nm. Typical performance for a different 1x2 filter is shown in Fig. 3 (b), with a larger extinction ratio of  $\sim 15$  dB, and a cutoff wavelength at 2120 nm. The cutoff wavelengths for the longer wavelength devices are displayed in Fig. 3 (c), where cutoffs from 2070 nm to 2160 nm were measured for steps of 8 nm increments of  $w_A$ . Finer control of the cutoff wavelength can be achieved by compensating the  $w_A$  increase by decreasing  $g_2$  or increasing  $w_B$ .

In general, although there are no fundamental limitations to device operation other than material loss, more than two TE modes at much shorter wavelengths can cause unwanted intermodal coupling, and reduce the extinction ratio. This can be prevented by a cascading 1x2 filters with different cutoffs into a multi-stage low-pass/band-pass/high-pass filter, where the resulting 1xN structures can be used in many photonics applications.

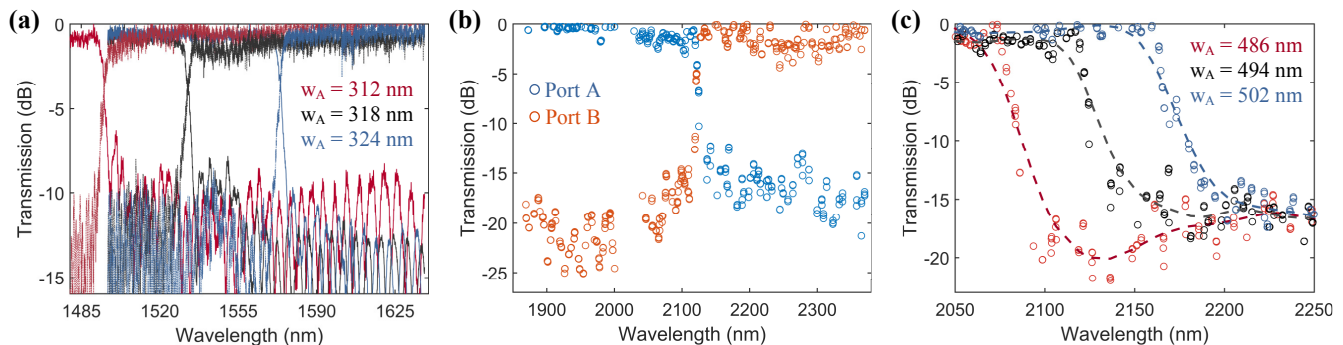


Fig. 3 Transmission spectra for output ports of the 1x2 filters with cutoffs around (a) 1550 nm, (b) 2150 nm, and (c) the resulting cutoff shift with changing  $w_A$ .

### 4. Conclusion

A robust and consistent methodology is developed for the design of mode-evolution-based, single cutoff, broadband, integrated 1x2 filters. The two-step design process uncouples the cutoff wavelength from the transition structures, and hence allows it to be accurately determined using only an eigenmode solver. Upon measurement of the fabricated devices, 15 dB extinction ratio has been demonstrated with less than 1 dB insertion loss; and filter roll-offs as high as 2.5dB/nm were recorded. This novel 1x2 port structure can add additional flexibility to integrated optical systems for broadband communication, sensing, supercontinuum or new frequency generation, all-optical signal processing, and other wavelength-division-multiplexing applications.

*This work was supported under the DARPA DODOS project, contract number HR0011-15-C-0056. The authors would like to thank Dr. Robert Lutwak for useful discussions.*

### References

- [1] Singh, Neetesh, et al. "Midinfrared supercontinuum generation from 2 to 6  $\mu\text{m}$  in a silicon nanowire." *Optica* 2.9 (2015): 797-802.
- [2] Wang, Cheng, et al. "Integrated high quality factor lithium niobate microdisk resonators." *Opt Express* 22.25 (2014): 30924-30933.
- [3] Uematsu, Takui, et al. "Design of a compact two-mode multi/demultiplexer consisting of multimode interference waveguides and a wavelength-insensitive phase shifter for mode-division multiplexing transmission." *Journal of Lightwave Technology* 30.15 (2012): 2421-2426.
- [4] Horst, Folkert, et al. "Cascaded Mach-Zehnder wavelength filters in silicon photonics for low loss and flat pass-band WDM (de-) multiplexing." *Opt Express* 21.10 (2013): 11652-11658.
- [5] Doerr, Christopher R., et al. "Monolithic InP multiwavelength coherent receiver using a chirped arrayed waveguide grating." *Journal of Lightwave Technology* 29.4 (2011): 536-541.
- [6] Wang, Xu, et al. "Narrow-band waveguide Bragg gratings on SOI wafers with CMOS-compatible fabrication process." *Opt Express* 20.14 (2012): 15547-15558.
- [7] Ghaffari, A., et al. "Photonic crystal power splitter and wavelength multi/demultiplexer based on directional coupling." *Journal of Optics A: Pure and Applied Optics* 10.7 (2008): 075203.
- [8] Stanton, Eric J., et al. "Multi-octave spectral beam combiner on ultra-broadband photonic integrated circuit platform." *Opt Express* 23.9 (2015): 11272-11283.